Water evaporation flux and cooling efficiency of spraying on cross-flow exchangers

S.O.L. Lacour, D. Flick, F. Trinquet, D. Leducq, P.E. Vende

Version of Record: https://www.sciencedirect.com/science/article/pii/S1359431120331343
Manuscript_39701a10fe0f10736ddfa25eae007f4d

Water evaporation flux and cooling efficiency of spraying on cross-flow exchangers

S.O.L. Lacour, D. Flick, F. Trinquet, D. Leducq, P.E. Vende

Universite Paris-Saclay, INRAE, UR FRISE, F-92761, Antony, France

*: corresponding author: stephanie.lacour@inrae.fr

June 9, 2020

Abstract

During heat waves, spraying heat exchanger helps to prevent overheating thermal processes like air conditioning systems. Spraying efficiency is studied to get the best performance enhancement ratio and avoid pressure drop related to water films. In this paper, we studied the effectiveness and local heat transfer coefficient for an exchanger which is partially sprayed. Thermography is used to describe wet section locations and areas for assessing incoming water flux. Results show an increase between 10 up to 30% of the local heat transfer coefficient in wet passes. On the opposite, global exchanger effectiveness is lowered to about 3% in wet conditions. This effect is related to the increase of the heat capacity on the air-side which reduces the calorific ratio in most cases. Spray cooling impact is most of the time limited by evaporation in the experiment. A formula is proposed to diagnose evaporation rate according to wall temperature, air humidity, and incoming water flux. It is also shown that effective evaporative cooling is shared between air and working fluid. Cooling transfer to working fluid depends on the calorific ratio between fluids. Hence, this latest affects spraying efficiency and has to be considered in optimizing spray cooling of heat exchangers.

Key words: heat exchanger effectiveness; spray cooling efficiency; calorific ratio; local evaporation rate

1 Introduction

If air is not saturated with water vapor, spraying water droplets in air flow decreases its temperature and intensifies heat transfer related to hot devices. Spraying a heat exchanger surface is therefore a possible method for improving its performance, especially when the temperature gradient between wall and air is small. This situation often occurs during heat waves and spraying may prevent overheating of processes during summer. Water management for spray cooling has received a growing attention these last years and recent works are mostly focused low spraying fluxes and their related efficiency ([1],[2],[3],[4]and[5]). Spraying efficiency has been studied in many papers in which a special attention is given to cooling efficiency of water and enhancement of heat transfer coefficient.

Spraying exchangers recovers in fact a two-step cooling. In a first step, an evaporative or adiabatic cooling is produced by droplet evaporation in air before reaching the heat exchangers. Droplet evaporation is in this case mainly limited by air temperature, humidity and residence time of droplets in air ([6], [7]). The cooling efficiency, that could be also called here the precooling efficiency, is in this case related to the difference between dry and wet bulk temperatures

([8]). More precisely, it is expressed by the ratio of effective air temperature drop to the difference between dry and wet bulk temperatures. This efficiency is generally higher if droplet residence time is long, what can be achieved with counter-flow water injections ([9], [10]). The humidification efficiency, i.e. the ratio between effective evaporated water and saturation vapor mass, is also sometimes introduced as in [11] and is useful for water management.Saturation air limits water evaporation during the precooling so that increasing water mass flow rate does not necessary improve the cooling effect and is sometimes not recommended ([12], [13]).

When air flow with non evaporated remaining droplets reaches hot walls, mixture temperature increases and so does the hygroscopic content of air. Water evaporation continues in the liquid film and in air for particles which are not collected at exchanger walls. The additional evaporation and collection rate were discussed in [14], [15] and [5], where experimental difficulties for separating these contributions were stressed. In spray cooling approaches, spray efficiency is expressed by the ratio between heat flux removed from the wall and the sum of sensible and latent flux corresponding to water spray heating and evaporating, according to Kim in [11]. Water film evaporation was deeply studied for cooling of steel where wall temperatures are very high and bubble nucleation occurs in the film. This application corresponds to the two phase regime described by Kim. In this regime, increasing water mass flow rate generally lead to increase the heat transfer ([16]) and ensure the boiling heat transfer method ([17]). This avoid drying surfaces and reaching then the critical heat flux. However, some authors suggest that mass flow rate should be adjusted to get a thin film and accelerate the renewal of water on the hot surface ([18]). Below 70 °C, the heat transfer mechanism is dominated by single phase convection. This regime received less attention in literature and Oliphant et al. in [19] reports controversies about evaporation role in non-boiling film heat transfer: he emphasizes that evaporation becomes dominant when the liquid to air mass flow ratio is low. Dreyer et al. in [20] presents a literature survey about the enhancement of heat transfer by spraying low water densities ($< 120 kg/m^2.h$). For electronics cooling applications, walls are often plates with various surface aspects, heated at constant flux conditions or fixed wall temperatures. Correlations for heat flux as well as heat exchange coefficients are generally determined, like in the papers [19], [21] and [22] [23] to predict the heat transfer in wet conditions.

For heat exchangers, geometries are more complex, especially when air flow crosses through hot walls. Fins are generally used to increase exchange area on the air side but these induce pressure drop and fouling problems ([24]). At walls, spray water film may cause flow blockage and add additional pressure drop ([25],[26]). Therefore, correlations for spraying on exchangers are generally established for both the Colburn factor, related to the air-side thermal coefficient, and the friction factor, related to pressure drop. The performance enhancement is usually defined by the ratio between heat fluxes in wet conditions and dry conditions ([1], [5], [21], [20], [25] and [27]). Some authors prefer to describe change in the heat exchange coefficients with a Colburn factor ratio ([14],[25]). The COP (coefficient of performance) is used instead of heat fluxes for condensers in refrigeration systems ([28], [29], [30]). Some authors assumed, like Walczyk in [31], that the performance enhancement coefficient is equivalent to the ratio of wet on dry global heat transfer coefficient. The enhancement ratios are most of the time preferred to spray efficiency for heat exchangers since they are easier to establish.

Spray mass balance and evaporation rate are in fact rarely studied in spraying heat exchanger because measurement of the latent energy balance of spray is very difficult to establish. Firstly, the real wet section is unknown because of the complex 3-dimensional geometries. Secondly, relative humidity changes are disturbed by pressure drop leading to uncertainties about vapor ratios in air. Thirdly, wall temperature evolves along the exchanger and heat exchange is not

at either fixed temperature or constant flux. Hence, spray balance is conversely used to determine the wet area. In the paper of Zhang et al. ([32]), the wet frontal area is derived from the wet and dry energy balance. Allais et. al. [14] used a specific experimental device to study spray collect on cylinders. They assessed the unknown wet area from the measurement of collected spray. They also shown that at low water flow rates, the performance enhancement ratio grows linearly with spray mass flow rate up to a critical value above which it stagnates. Zhang et al. also presented similar results in [32] and stressed the asymptotic behavior of total capacity at large spray flow rates. Vende et al. in [26] also suggested that a threshold value of spray flow rate could explain clogging occurrence. These findings indicate that an optimal water spray rate exists for evaporative cooling on heat exchangers and could be studied with information about wet area, local wall temperatures and evaporation balance.

This paper presents a study about local evaporation rate and its impact on local heat transfer coefficients on a cross flow heat exchanger. First, the global impact of spraying is stated on temperature profiles and heat transfer effectiveness. Heat transfer coefficient are then studied at a local and global scale. Thanks to infra-red thermography and image analysis, wet sections are measured to determine the incoming spray flux and local evaporation rate is deduced from energy conservation. Spray cooling budget is discussed regarding the heat capacity ratio of fluids. An expression is also proposed to determine the critical spray flux as a function of dry wall temperature, wet area and ambient humidity.

2 Experimental Method

An experimental device is used to characterize heat transfer enhancement of water spraying on a heat exchanger. This device is located in a climatic room where ambient temperature and humidity are constant during test. It is composed of a heat exchanger on which a spraying system is fixed. An IR camera is used to assess impacted sections on heat exchanger.

2.1 Air/Water heat exchanger

The heat exchanger is a typical HVAC condenser used for air conditioning in automotive applications and cools the working fluid (here, water) with air. The heat exchanger is a four-pass flat-tube heat exchanger in aluminum represented in Fig. 1. Its transverse section is 516 mm long and 396 mm height for 12 mm of depth. Rectangular tubes are divided into 5 microchannels.The number of tubes per pass varies from 16 down (pass 1) to 12 (pass 2), 8 (pass 3) and 6(pass 4) tubes so the water velocity and internal heat transfer coefficient vary for each pass. Louver fins are disposed between tubes and have the same depth. More details about exchanger geometry are given in [26]. Inside the heat exchanger, water (water is the so-called working fluid in the following) flows thanks to 10 kW temperature control unit Vulcatherm 10805, that can deliver flow rates between 275 and 580 L/h (flowmeter Endress& Hauser Promag 50H,$\pm$ 0.5% of accuracy) at a regulated inlet temperature from 40 to 70 °C. Temperature sensors are put on lateral flanges in the middle of each pass. A fan is located just after the exchanger and sucks air through a tube where air outlet temperature is measured. This tube allows temperature and air flow rate monitoring. Fan speed is controlled by an fixed tension at the fan engine and a tachymeter is used for measuring fan rotation speed, converted into air flow rate using a calibrated regression (Tachymeter ALMEMO, accuracy $\pm$ 0.02% of accuracy). Relative humidity and ambient temperature are monitored with hygrometers (Vaisala HMP110, accuracy $\pm$ 1.5 % for RH and $\pm$ 0.2°C for T) and temperature sensors respectively (Thermocouple Type T for walls, accuracy $\pm$ 0.13 °C and PT100 for water and

air temperatures, $\pm$ 0.1°C) were calibrated before their installation. As hygrometers show deviations between inlet and outlet, even in dry cases, they were not used to study the cooling spray balance. Indeed, 1.5% of uncertainty on the relative humidity correspond to 14% on the vapor ratio, which represents more than a half of the spray flow rate.

2.2 Spraying system

The spraying system is composed of one of three atomizers described hereafter, a 15 L bottle of stored water and a pump. The pump (Prominent beta b, up to 25 bar) brings water from the bottle to the atomizer that expands it into spray. Spray pressure and temperature are monitored and spray water flow rate is obtained weighing continuously the storage tank (Mettler PE24, $\pm$ 2g of accuracy). Three hollow-cone nozzles are used in the present experiment (LECHLER type 220.004 equipped with 0.1 mm diameter hole, type 220.014 with 0.15 mm diameter hole and type 212.085 with 0.25 mm diameter hole). Nozzle bodies are fixed near the exchanger on 2 positions: position 1 (hole position: x=-40,y=40,z=185 mm) is on the lateral side of the exchanger with the nozzle spraying cross-flow. Position 2 (hole position: x=-70,y=90,z=370 mm) is on the top of the heat exchanger, nozzle pointing at the ground and farther from wall, as shown in the Fig. 1. As nozzles are very closed to the exchanger, the precooling effect of air is not be addressed separately from those of the direct spraying effect. Both nozzle type and pressure are used to control the spray flow rate which varies between 0.7 and 2.1 L/h. Cross-flow injection ensures a partial wetting of exchanger section and keep all the spray flow rate in the monitored domain.

2.3 Impacted section

An infrared camera (ThermaCAM FLIR E45) is located at 1.6 m in front of the heat exchanger. During the test, one picture is taken before spraying and then, pictures are taken every 10 s during spraying. In a previous work ([26]), a thermal image analysis was developed to determine where is the water location on the heat exchanger. It lies on the following steps:

1. matching and subtraction of the heat exchanger background (image without spraying),
2. gray-scaling to process further image analysis,
3. mask applied to the Fast Fourier Transform in order to remove interference noise of exchanger tubes,
4. Gaussian Blur to smooth the remaining noise,
5. Otsu's method to binarize the image.

The output of binarization gives the amount of changed pixels with and without spraying and are converted into square meters to find out the wet (or impacted) section. It is to notice that the impacted section is a frontal section reflecting incident water fluxes. It differs from the wet area used by Allais et al. ([14]) on the cylinder because the percentage of wet area inside fins is not known. The wet section is always smaller than heat exchanger dimensions. Therefore, we assumed that the whole water fluxes go through the wet section and they are no water loss in surrounding. It is explained in [26] that the wet section firstly grows and reachs a stable value after 5 minutes of spraying. After ten minutes, the wet section may be dissociated in a constant efficient cooling section and a total wet section: the total wet section may increase after 10 minutes because the liquid water stored in fins starts to rainout in some cases. Here, we

used only the first 10 minutes, when efficient cooling section and total wet section are stacked. Wet section stability was controlled and 3 tests with time varying sections were rejected from the present analysis.

2.4 Test procedure

Objectives of these measurements are assessing the energy balance of spray and heat exchanger, what is done by comparing wet and dry conditions. Hence, all the wet conditions are paired with dry conditions recorded just before starting spraying. When thermal equilibrium is reached in dry conditions, recording data starts during 10 minutes and then, spray is switch on for at least 10 minutes. Data, sampled every 5 s, are averaged over the last 5 minutes of each period to characterize the steady state balance. 36 tests were used in the analysis. These include change of spray flow rate, nozzle type, nozzle position, working fluid and air flow rates, inlet working fluid temperatures. Ambient conditions were monitored but not controlled, so that air temperature varies between 23 and 25 °C and relative humidity between 30 and 50% among tests.

3 System energy analysis

The analysis of measurement lies on the energy balance inside the heat exchanger. Rather than the usual enthalpy slope used in [25], the apparent calorific value used by Hsu et al. in [33] is used to express results in the heat exchanger framework, using the number of transfer unit method. Equations are described in the following.

3.1 Exchanger energy balance

Assuming negligible thermal losses in the air tunnel, energy balance ensures in dry conditions that:

$$m_a.C_{p,a}.(T_{a,o,d} - T_{a,i,d}) \quad = \quad m_f.C_{p,f}.(T_{f,i,d} - T_{f,o,d}) \tag{1}$$

where m is the massic rate, C_p the calorific heat at constant pressure and T temperature at inlet (i) and outlet (o) for air (a) and working fluid (f). In wet conditions, this has to be rewritten in terms of enthalpy for the air because of the latent contribution of spray evaporation. The mixture total enthalpy H_t is then written with and being zero at $T_{ref} = 0$ °C:

$$H_t \quad = \quad m_a.C_{p,a}.T_a + m_a.y_a(C_{p,v}.T_a + \Delta H_{vap}) + m_l.C_{p,l}.T_l \tag{2}$$

where H_{vap} is the latent heat of vaporisation. The spray mass conservation is written by summing vapor (v) and liquid (l) content:

$$m_s \quad = \quad m_l + m_v = m_l + m_a.\,(y_{a,o} - y_{a,i}) \tag{3}$$

Combining enthalpy difference between the inlet and outlet (Eq. 2), heat exchanger energy balance (Eq. 1 and spray mass conservation (Eq. 3), it comes the outgoing vapor ratio $y_{a,o}$ corresponding to the following equation:

$$\begin{aligned} y_{a,o} \quad &= \quad [m_f.C_{p,f}.(T_{f,i,w} - T_{f,o,w}) - m_a.C_{p,a}.(T_{a,o,w} - T_{a,i,w}) \\ &+ \quad m_a.y_{a,i}.(C_{p,v}.T_{a,i} + \Delta H_{vap} - C_{p,l}.T_l) - m_s.C_{p,l}.(T_l - T_{s,i})] \\ &/ \quad [m_a.(C_{p,v}.T_{a,o} + \Delta H_{vap} - C_{p,l}.T_s - C_{p,l}.T_s)] \end{aligned} \tag{4}$$

In Eq. 4, T_l is the temperature for liquid water going out of the system. m_l refers to the liquid content, which is either stored inside exchanger fins nor going outside with air because water droplets were not collected by the exchanger. As no drainage was observed outside on the exchanger during tests, we assumed that the liquid content is mainly stored in water film between fins at wall temperature. Indeed, IR images show these accumulations and our experiments were even used to study clogging in [26]. The wall temperature is determined using a linear approximation of the temperature gradient on the pass where the barycenter of impacted section is located. Densities and specific heat at constant pressure are computed from pressure, temperatures and moisture contents using HAPropSI python routines of Coolprop (see [34]) for humid air, whereas PropSI with fluid as IF97::Water is used for the water spray and fluid in the exchanger.

The $C_{p,equi}$ method is used to rewrite the air-side balance using wet temperatures, so that effectiveness relations for heat exchanger can be used with temperature gradient in the same way as [33]:

$$C_{p,equi} = \frac{H_{a,o} - H_{a,i}}{T_{a,o,w} - T_{a,i}} \tag{5}$$

Eq. 5 shows that spray cooling amounts to increase the heat capacity of air. The heat capacity ratio is a key parameter for exchanger design (see [35]) and is written here using the equivalent calorific rate $C_{p,equi}$ only for wet conditions:

$$R = \left[\frac{m_a.Cp_a}{m_f.Cp_f}\right]_d = \left[\frac{m_a.Cp_{p,equi}}{m_f.Cp_f}\right]_w \tag{6}$$

The Z ratio is also a heat capacity ratio, but varies between $[0, 1]$ because it accounts for heat transfer limitations related to fluid thermal properties:

$$Z = \frac{(m.C_p)_{min}}{(m.C_p)_{max}} \tag{7}$$

Most of the time, air is the limiting fluid in our experiments but the working fluid also limits the exchange in 3 of the tests with dry conditions and 5 of the tests in wet conditions.

3.2 NTU and exchanger effectiveness

The effectiveness ϵ, is the ratio between the actual q and the maximum possible q_{max} heat transfer rate, this latest being $q_{max} = (m.C_p)_{min}.(T_{f,i} - T_{a,i})$.

$$\epsilon = \frac{q}{q_{max}} = \frac{1}{R}.\frac{T_{f,i} - T_{f,o}}{T_{f,i} - T_{a,i}} \text{ if } R < 1 \tag{8}$$

$$\epsilon = \frac{T_{f,i} - T_{f,o}}{T_{f,i} - T_{a,i}} \text{ if } R > 1 \tag{9}$$

The number of transfer units is related to the heat capacity ratio Z and effectiveness through an expression which depends on the exchanger geometry. For cross-flow exchangers, the most commonly used formula is found in [36] or [37].

$$\epsilon = 1 - \exp\left(\frac{NTU^{0.22}}{Z}.\left(\exp\left(-Z.NTU^{0.78}\right) - 1\right)\right) \tag{10}$$

Hence, the number of transfer units of the exchanger NTU can be computed from flow and temperatures measurement by solving Eq. 10. A global heat transfer coefficient can then be derived from the number of transfer units as:

$$NTU = \frac{K_{ex}.S_{ex}}{(m.C_p)_{min}} \tag{11}$$

The same procedure is applied to evaluate local heat transfer coefficient using the temperature profile obtained for the working fluid in each pass and using the same hypothesis as Fakheri in [38].

3.3 Energy and mass balance of spray

Evaporation rate sizes the effective cooling added through the spray and the wide variety of experiments was used to study it. Here, evaporation rate has to be studied at the local scale, regarding spray mass balance only over the impacted section. Here, the incoming total water content $y_{twc,loc}$ is assessed from air and spray flow contributions introducing the ratio of wet section S_s to whole exchanger section S_{ex}. It comes:

$$y_{twc,loc} = y_{a,i} + \frac{m_s}{m_a}.\frac{S_{ex}}{S_s} \quad (12)$$

In this expression, air velocity is supposed to be uniformly distributed in spray section as well as in dry area. The area ratio allows to size air flow rate in the wet section. The $(y_{twc,loc} - y_{a,i})$ represents the local water availability for evaporation. The effective outgoing vapor $y_{a,o,loc}$ ratio is assessed by introducing the effective vaporized flow rate:

$$y_{a,o,loc} = y_{a,i} + (y_{a,o} - y_{a,i}).\frac{S_{ex}}{S_s} \quad (13)$$

$(y_{a,o,loc} - y_{a,i})$ is the local vapor ratio added to air by evaporation and is linked to the evaporation rate τ_{evap}

$$\tau_{evap} = \frac{y_{a,o,loc} - y_{a,i}}{y_{twc,loc} - y_{a,i}} \quad (14)$$

$\tau_{evap}.m_s$ defines the effective evaporation rate. As the spray section is limited, local water availability often exceeds air evaporative capacity. Hence, τ_{evap} is interpreted as the critical spray rate, i.e. the maximal flux that has and can be evaporated. The spray flux was completely evaporated only in 2 tests and hence, we assumed that conditions are outside the linear growing of performance enhancement with water rate and always with water excess.

Evaporation limit decreases when wall temperatures and air hygroscopic capacity increase. In the paper [14], a critical spray rate is defined using the Chilton-Colburn analogy to assess the occurrence of water excess on hot cylinders:

$$m_{crit} = \frac{K_{cyl}}{C_{p,a}}.S_s.(y_{sat}(T_w) - y_{sat}(T_{a,i})) \quad (15)$$

Beyond the critical flux, improvement of wet heat exchange coefficient doesn't grow with the spray flow rate. Its expression depends on wall temperatures but also on the wet area and heat transfer coefficient in dry conditions K_{cyl}. The expression proposed by Allais et al. was tested in this work but gave evaporation rate much above observations. This might be due to difficulty in using frontal wet sections and global exchange coefficients instead of determining local heat transfer coefficients nor real wet area: geometry of fins is too complex to handle these local variables. The higher the wall temperature and the lower the inlet air humidity are, the higher the evaporation rate is. Therefore, we suggest the following approximation for estimating the outgoing vapor ratio by modeling $y_{a,o,m}$:

$$y_{a,o,m} = y_{sat,adia}(T_{wall,dry}, y_{a,in}) \quad (16)$$

The modelled evaporation rate may then be estimated from Eq. 16 using only measurements obtained in dry conditions. It sizes the effective spray cooling. The global vapor content of air can be retrieved from Eq. 17 assuming there are no change in the vapor ratio in dry zones, so that:

$$y_{a,o} = y_{a,i}(1 - \frac{S_s}{S_{ex}}) + y_{a,o,m}\frac{S_s}{S_{ex}} \quad (17)$$

The energy balance of the spray is now written by subtracting the wet from dry energy balance of the heat exchanger. As inlet condition are similar for wet and dry conditions, it comes:

$$\begin{aligned} m_a.(y_{a,o,w} - y_{a,i}).\Delta H_{vap} &= P_e = m_f.C_{p,f}.(T_{f,o,w} - T_{f,o,d}) + m_a.(y_{a,o,w} - y_{a,i}).C_{p,l}.T_{l,w} \\ &- m_s.C_{p,l}.(T_l - T_s) - ((C_{p,a} + y_{a,o}.C_{p,v}).T_{a,o,w} - (C_{p,a} + y_{a,i}.C_{p,v}).T_{a,o,d}) \end{aligned} \quad (18)$$

The term on left represents the effective cooling of spray, i.e. the latent power absorbed through its evaporation. Its optimal value, i.e. the cooling potential of the spray, corresponds to a complete evaporation and is given by $\Delta H_{vap}.m_s$. The effective cooling is used for cooling the working fluid, but also the air flow and liquid content. Hence, the energy budget of spraying is distributed into the following contributions, related to respectivelely fluid cooling P_f , air cooling P_a, inlet liquid cooling $P_{liq,i}$ and liquid storage P_{liq}:

$$P_e = m_a.(y_{a,o,w} - y_{a,i}).\Delta H_{vap} \quad (19)$$

$$P_f = m_f.C_{p,f}.(T_{f,o,w} - T_{f,o,d}) \quad (20)$$

$$P_a = m_a.\left((C_{p,a} + y_{a,o}.C_{p,v}).T_{a,o,w} - (C_{p,a} + y_{a,i}.C_{p,v}).T_{a,o,d}\right) \approx m_a.C_{p,a}(T_{a,ow,} - T_{a,od}) \quad (21)$$

$$P_{liq,i} = m_s.C_{p,l}.(T_l - T_s) \quad (22)$$

$$P_{liq,stored} = m_a.(y_{a,o} - y_{a,i}).C_{p,l}.T_{l,w} \quad (23)$$

$\tau_f = P_f/P_e$ is the part of latent energy devoted to cooling the working fluid and $\tau_a = P_a/P_e$ corresponds to air cooling. The performance enhancement ratio is related to τ_f and optimized spraying should be obtained by reducing the liquid storage and also τ_a. Experimental measurements are now used to express global effectiveness, heat transfer coefficients and evaporation rate during experiments.

4 Results

Measurements are used to study energy balance of heat exchanger and spray. A preliminary analysis has been performed to check for measurement accuracy. First, the energy balance of air has been compared to the working fluid energy balance under dry conditions. The difference in dry balances has a maximal value of 11% and a dispersion coefficient of 3.6%. Inlet temperatures and flow rates are also compared in both dry and wet conditions: the maximal difference is observed for air flow rate and its variation is below 3.5%. This analysis shows the good agreement of conditions in wet and dry cases, allowing the sizing of evaporation in wet cases from the energy balance.

4.1 Fluid temperature profile along the exchanger

A typical temperature profile is obtained for working fluid whose temperature decreases along the exchanger, as shown in Fig. 2. In wet cases, temperature at outlet is always below the one of its corresponding dry case. The temperature difference $T_{f,o,d} - T_{f,o,w}$ for working fluid is higher than sensor accuracy, with a mean around 0.9°C and a minimal at 0.2°C. It is to notice that air outlet temperature is lowered in wet cases. The performance enhancement ratio, written $(T_{f,o,w} - T_{f,o,d})/T_{f,o,d}$, is about 7% in average, with a standard deviation of 3.8% on the whole set of tests. Air temperature difference $T_{a,o,d} - T_{a,o,w}$ is just above those of working fluid with 1°C in average. This shows that spray evaporation does not only cool the working fluid, but also has a sensible cooling effect on airflow. This air cooling was also noticed by Wang and al. ([29]) who reported 5°C less for wet air at a condenser outlet.

4.2 Global effectiveness of Air/Water exchanger

The equivalent C_p is computed for wet conditions and varies from 1040 up to 1305 kJ/kg.K, with 1150 in average, whereas it is about 1020 kJ/kg.K in dry conditions. So evaporation increases the specific heat capacity of air. Changing

the capacity ratio of fluids has consequence on the global effectiveness of heat exchangers: the more the Z ratio increases, the less heat exchanger effectiveness is. This is shown in Fig. 3 where exchanger theoretical effectiveness is reported according to the NUT for various Z ratio. Experimental results, colored by their Z ratio category, are also reported in this figure. Increasing air capacity leads to increase the capacity ratio of the heat exchanger, as air is most of the time the limiting fluid. This induces a decrease of the exchanger effectiveness, what is shown by the slight displacement on the bottom for wet points (stars) compared to dry points (squares). The effectiveness change is about 3% in average. The only situation where it grows is when water becomes the limiting fluid (black points). This is the only case where spraying increases exchanger effectiveness. NTU numbers are very similar for both conditions.

4.3 Local heat transfer coefficients

The global heat transfer coefficient is deduced from the number of unit transfer derived from effectiveness and capacity ratio. The NTU is similar in wet and dry cases but global heat transfer coefficient raises, as it is re-multiplied by $(m.C_p)_{min}$. The global heat transfer coefficient is increased of about 11% for position 1 and 5% for position 2. In fact, it varies proportionally with the performance enhancement ratio and is about 8% when averaging all cases,i.e. near the performance enhancement ratio. Due to the partial spraying, enhancement is small compared to usual magnitude(50 % in [27] or [31] and more than 200% in [1],[14]). This is because only 13% in position 1 (respectively 7% in position 2) of the section is wet In Fig. Local wet and dry coefficients are compared in Fig. 4(c), whereas impacted section are reported in Fig. 4 (a) and (b). Spray impacts at different locations according to nozzle position. Air flow rate and injection pressure slightly modify impacted sections but the barycenter of wet sections stays nearly always at the same place. In position 1, wet section average is about 265 square centimeters and water density varies from 65 up to 120 $Kg/m^2/h$ according to injection pressure. In position 2, wet section average is lower, about 145 square centimeters. This is because we used only the nozzle with the smallest hole for this position. As water rate is also lowered with small hole, spray density stays however in the same range as for position 1. It was not possible to adjust wet area on only one pass and hence, wet area for each pass was obtained by triangulation. For position 1, we found that 5% of the impacted section is on pass 1, 83 % on pass 2 and 12% on pass 3. These values are averaged on all tests. In position 2, 64% of the wet section is on pass 1 and 36 % on pass 2. The pass 4 is never impacted by the spray. Then, local heat transfer coefficients are computed for each pass. Looking back at Fig. 4(c), it is confirmed that for wet passes ,i.e. pass where the spray impacts, the heat transfer coefficient always increases: For position 1, the local coefficient raises significantly of 23% on pass 2 and of 19% on pass 3. For position 2, it raises significantly of 4% on pass 1 and of 21% on pass 2. This shows that the augmentation does not correspond to wet section proportion. Amazingly, the heat transfer coefficient is reduced for pass 3 in position 2: this may be related to a lower temperature gradient between air and fluid in wet conditions compared to dry ones. But, local heat transfer coefficients are unchanged outside of the impacted passes (pass 4), as expected.

4.4 Evaporation rate assessment

Spray densities are nearly the same for all nozzles, around 80 $kg.m^{-2}.h^{-1}$, what is in the same range as Nazarov in [3] and much lower than Zhang in [32]. It was found difficult during experiments to control precisely the spray flow rate with the pressure: fouling in the nozzle may disturb the relation between pressure and spray flow rate at low pressure. The evaporation rate varies from 25% up to 100% during tests, with a mean value at 55%. It increases when

working fluid temperature increases and presents higher values for nozzles in position 2. Indeed, spray impacts the hottest pass for this position. This show that high evaporation rate does not correspond to the highest enhancement because of the smallest wet section. In Fig 5(a), the outgoing vapor ratio $y_{a,o}$ is reported according to the total incoming water content y_{twc} and the $y_{twc} = y_{twc}$ line is also shown. Stars on this line means that all the incoming water content exits as vapor and spray has been completely evaporated. It is to notice that evaporation was limited to the available water content during calculations and that's why no star are above the line. A few points lies near or on the line but most of the time, spray flux was above what could be evaporated. The distance from the line represents the remaining content staying in liquid state. Distant points are often found for high incoming water content: spray fluxes were too high. Elevated evaporation rate are generally observed for intermediate incoming water content and the figure shows that. However, in few cases, high liquid content (distant points) are even observed for low incoming water content. These cases are generally related to low working fluid temperatures. On heat exchanger, as wall temperature varies, local evaporation rate varies and spray rate has to be adapted to the position. Model of evaporation rate is needed to determine the optimal and local spray rate.

In Fig. 5(b), the modelled outgoing vapor ratio $y_{a,o,m}$ is reported according to the observed one, $y_{a,o,m}$. This figure shows that the Eq. 16 gives an acceptable forcast of the vapor ratio at the exit reproducing the general trend for the evaporation rate. However, the correlation between model and measurement is above 0.86 ($R^2 = 0.75$) revealing the critical flux model has to be further improved. But uncertainties about wet sections are rather high: values are generally contained in the $\pm$ 20% of a linear trend between spray flow rate and wet section. 15 % difference on wet sections are commonly observed for tests with similar nozzle, pressure and air conditions. Such uncertainties prevent the improvement of the model yet. However, the formula helps to diagnose critical spray flux and can be used with moving nozzle strategies, as in [18].

4.5 Effective latent energy for cooling fluids

The power analysis is made computing the enthalpy rate of the liquid water introduced with the nozzle. The spray flow rate is converted into cooling potential, which corresponds to the amount of power required for evaporating all the spray. Effective cooling is assessed from the effective evaporation rate by Eq. 19. Effective cooling is shared between air (Eq. 21 and working fluid (Eq. 20 and the ratio of air to fluid cooling is presented in the last column of the Table 1. Water enthalpy rate at the nozzle varies according to the spray flow rate from 25 up to 90 W according to tests: as the pressure scales the flow rate, it has a direct impact on this power. The reader should be aware that this power is related to the thermodynamic enthalpy of water, depending on injection pressure and temperature: it does not take into account for the pump efficiency. If all the spray could evaporate, the cooling potential power of the spray should be comprised between 500 up to 1500 W. The effective cooling power lies in fact between 260 up to 880 W, what corresponds to an average evaporation rate of 50% find in the previous paragraph. The power staying in the remaining liquid content is small compared to contributions for air and fluid cooling: its value varies a lot with the hypothesis about the liquid temperature ($\pm$ 40% from $T_{air,in}$ up to $T_{f,in}$) but it always stays considerably less than the cooling power for other fluids. Both fluids are cooled by about 250 W in average, but in fact the share of cooling varies widely according to tests. Air cooling is not negligible and sometimes overheads largely working fluid cooling.

The cooling balance of spray is made by comparing the latent effective cooling, related to evaporation rate, to measured sensible coolings of working fluid and air. The first one comes from the energy balance of heat exchanger whereas

the second is given by comparing wet and dry temperatures at outlet. The comparison is represented on Fig. 6(a) and shows that the balance often stays out of the $\pm 10\%$ range generally awaited: the spray balance is less accurate than those for the heat exchanger because powers involved in the spray balance are much lower than heat exchanger power. Therefore, the spray balance is more sensitive to measurements uncertainties. However, the agreement is found acceptable with regards the amount of tests. On Fig. 6(b), it is shown that the calorific ratio is the best explanation for sharing the latent cooling between fluids. When working fluid is the limiting fluid in exchanger, water resists to cooling and cold is preferably transferred to air. On the opposite, when air is the limiting fluids, cold is rather transferred to working fluid and not to air. As the performance enhancement ratio directly sizes the heat transferred to the working fluid, it is shown that the calorific ratio of the exchanger plays a role on the performance ratio. It also explains why important performance enhancement ratio can be expected for condensers, where the calorific ratio tends near zero.

5 Conclusion

The performance enhancement ratio of partial spraying on a exchanger is about 7% on average over all the tests. Spray evaporation increases the heat capacity rate of air in wet conditions. As the NTU are almost equal in wet and dry conditions, exchanger effectiveness is reduced from about 3% with spraying. The global heat transfer coefficient, increased of about 8% when averaging all cases, is affected by nozzle positions. In wet passes, the local heat transfer coefficient increases much more but in a proportion somewhat independent of spray density. High evaporation rates are generally obtained for intermediate spray density and high wall temperature. As spray densities were most of the time above what could be evaporated, a formula is derived from results to adjust spray density to evaporation potential. The cooling balance of spray is made by comparing the latent effective cooling to sensible cooling of working fluid and air. Air cooling is not negligible and sometimes overheads largely working fluid cooling. Expressing thermal resistance to transfer, the calorific ratio drives the share of cooling between fluids. As the performance enhancement ratio directly sizes the heat extracted from the working fluid, it is found that the calorific ratio plays a role in the performance ratio.

Acknowledgments

The authors are grateful for the financial support provided by the ADEME (Agence De l´ Environnement et de la Maîtrise de l´ Energie) in the context of the EfficAC project number 1482C0178. The authors also thank Renault and Valeo for lending equipment for experiments.

References

[1] C.-W. Chen, C.-Y. Yang, Y.-T. Hu, Heat transfer enhancement of spray cooling on flat aluminum tube heat exchanger, Heat Transfer Engineering 34 (1) (2013) 29–36. doi:10.1080/01457632.2013.694742.

[2] S. Popli, Y. Hwang, R. Radermacher, Performance enhancement of enhanced herringbone wavy-fin round tube inclined heat exchangers with and without hydrophilic coating using evaporative spray and deluge cooling, in: Proceedings of the ASME International Mechanical Engineering Congress and Exposition, 2013, vol 8b, ASME, 2013, aSME International Mechanical Engineering Congress and Exposition (IMECE2013), San Diego, CA, NOV 15-21, 2013, Article number-V08BT09A035.

[3] A. D. Nazarov, A. F. Serov, V. I. Terekhov, The influence of gas coflow in a pulse aerosol on evaporation cooling process, High Temperature 52 (4) (2014) 576–579. doi:10.1134/S0018151X14040178.

[4] C.-N. Huang, Y.-H. Ye, Development of a water-mist cooling system: A 12,500 kcal/h air-cooled chiller, Energy Reports 1 (2015) 123–128. doi:10.1016/j.egyr.2015.04.002.

[5] L. Xiao, T. Wu, S. Feng, X. Du, L. Yang, Experimental study on heat transfer enhancement of wavy finned flat tubes by water spray cooling, International Journal of Heat and Mass Transfer 110 (2017) 383–392. doi:10.1016/j.ijheatmasstransfer.2017.03.054.

[6] R. Belarbi, C. Ghiaus, F. Allard, Modeling of water spray evaporation: Application to passive cooling of buildings, Solar Energy 80 (12) (2006) 1540–1552.

[7] J. Tissot, P. Boulet, F. Trinquet, L. Fournaison, H. Macchi-Tejeda, Air cooling by evaporating droplets in the upward flow of a condenser, International Journal of Thermal Sciences 50 (11) (2011) 2122–2131.

[8] M. Lemouari, M. Boumaza, Experimental investigation of the performance characteristics of a counterflow wet cooling tower, International Journal of Thermal Sciences 49 (10) (2010) 2049–2056.

[9] S. Hamlin, R. Hunt, S. A. Tassou, Enhancing the performance of evaporative spray cooling in air cycle refrigeration and air conditioning technology, Applied Thermal Engineering 18 (11) (1998) 1139–1148.

[10] J. Tissot, P. Boulet, A. Labergue, G. Castanet, F. Trinquet, L. Fournaison, Experimental study on air cooling by spray in the upstream flow of a heat exchanger, International Journal of Thermal Sciences 60 (2012) 23–31. doi:10.1016/j.ijthermalsci.2012.06.005.

[11] J. H. Kim, Spray cooling heat transfer: The state of the art, International Journal of Heat and Fluid Flow 28 (4) (2007) 753–767.

[12] Y. Yang, L. Yang, X. Du, Y. Yang, Pre-cooling of air by water spray evaporation to improve thermal performance of lithium battery pack, Applied Thermal Engineering 163. doi:10.1016/j.applthermaleng.2019.114401.

[13] W. Ye, Q. Zhang, Y. Xie, J. Cai, X. Zhang, Spray cooling for high temperature of exhaust gas using a nozzle array in a confined space: Analytical and empirical predictions on cooling capacity, Applied Thermal Engineering 127 (2017) 889–900. doi:10.1016/j.applthermaleng.2017.08.097.

[14] I. Allais, G. Alvarez, D. Flick, Analyse du transfert thermique entre un cylindre et un écoulement dáir faiblement chargé en gouttelettes déau, Revue Générale de Thermique 36 (4) (1997) 276 – 288. doi:https://doi.org/10.1016/S0035-3159(97)80688-5.

[15] P. Boulet, J. Tissot, F. Trinquet, L. Fournaison, Enhancement of heat exchanges on a condenser using an air flow containing water droplets, Applied thermal engineering 50 (1) (2013) 1164–1173.

[16] M. C. Riofrio, N. Caney, J.-A. Gruss, State of the art of efficient pumped two-phase flow cooling technologies, Applied Thermal Engineering 104 (2016) 333–343. doi:10.1016/j.applthermaleng.2016.05.061.

[17] Y. Wang, Y. Jiang, W. Chen, B. Zhou, Heat transfer characteristics of spray cooling beyond critical heat flux under severe heat dissipation condition, Applied Thermal Engineering 123 (2017) 1356–1364. doi:10.1016/j.applthermaleng.2017.04.165.

[18] O. Lamini, R. Wu, C. Y. Zhao, Z. G. Xu, Enhanced heat spray cooling with a moving nozzle, Applied Thermal Engineering 141 (2018) 921–927. doi:10.1016/j.applthermaleng.2018.06.025.

[19] K. Oliphant, B. Webb, M. McQuay, An experimental comparison of liquid jet array and spray impingement cooling in the non-boiling regime, Experimental Thermal and Fluid Science 18 (1) (1998) 1–10. doi:10.1016/S0894-1777(98)10013-4.

[20] A. Dreyer, D. Kriel, P. Erens, Analysis of spray cooled finned-tube heat exchangers, Heat Transfer Engineering 13 (4) (1992) 53–71. doi:10.1080/01457639208939788.

[21] M. Kim, C. Bullard, Air-side performance of brazed aluminum heat exchangers under dehumidifying conditions, International Journal of Refrigeration-Revue Internationale du Froid 25 (7) (2002) 924–934. doi:10.1016/S0140-7007(01)00106-2.

[22] Y. Wang, M. Liu, D. Liu, K. Xu, Heat flux correlation for spray cooling in the nonboiling regime, Heat Transfer Engineering 32 (11-12) (2011) 1075–1081, 6th International Symposium on Multiphase Flow, Heat Mass Transfer and Energy Conversion, Xian, PEOPLES R CHINA, JUL 11-15, 2009. doi:10.1080/01457632.2011.556505.

[23] N. Zhou, F. Chen, Y. Cao, M. Chen, Y. Wang, Experimental investigation on the performance of a water spray cooling system, Applied Thermal Engineering 112 (2017) 1117–1128. doi:10.1016/j.applthermaleng.2016.10.191.

[24] R. Webb, N. Kim, Principles of enhanced heat transfer, second edition, Heat Transfer, Taylor & Francis, 2005.

[25] N.-H. Kim, S.-H. Kim, Dry and wet air-side performance of a louver-finned heat exchanger having flat tubes, Journal of Mechanical Science and Technology 24 (7) (2010) 1553–1561. doi:10.1007/s12206-010-0409-1.

[26] P. E. Vende, F. Trinquet, S. Lacour, A. Delahaye, L. Fournaison, Efficiency of water spraying on a heat exchanger: Local characterization with the impacted surface, Applied Thermal Engineering 128 (2018) 684–695. doi:10.1016/j.applthermaleng.2017.09.031.

[27] Y.-G. Park, A. M. Jacobi, The air-side thermal-hydraulic performance of flat-tube heat exchangers with louvered, wavy, and plain fins under dry and wet conditions, Journal of Heat Transfer-Transactions of the ASME 131 (6). doi:10.1115/1.3089548.

[28] M. Youbi-Idrissi, H. Macchi-Tejeda, L. Fournaison, J. Guilpart, Numerical model of sprayed air cooled condenser coupled to refrigerating system, Energy and Conversion Management 48 (7) (2007) 1943–1951.

[29] T. Wang, C. Sheng, A. G. A. Nnanna, Experimental investigation of air conditioning system using evaporative cooling condenser, Energy and Buildings 81 (2014) 435–443. doi:10.1016/j.enbuild.2014.06.047.

[30] F. W. Yu, K. T. Chan, Improved energy performance of air-cooled chiller system with mist pre-cooling mist improvement on air-cooled chillers, Applied Thermal Engineering 31 (4) (2011) 537–544. doi:10.1016/j.applthermaleng.2010.10.012.

[31] H. Walczyk, Enhancement of heat-transfer from air-fin coolers with water spray, Chemical Engineering and Processing-Process Intensification 32 (2) (1993) 131–138. doi:10.1016/0255-2701(93)85022-8.

[32] F. Zhang, J. Bock, A. M. Jacobi, H. Wu, Simultaneous heat and mass transfer to air from a compact heat exchanger with water spray precooling and surface deluge cooling, Applied Thermal Engineering 63 (2) (2014) 528–540. doi:10.1016/j.applthermaleng.2013.11.046.

[33] S. Hsu, Z. Lavan, W. Worek, Optimization of wet-surface heat-exchangers, Energy 14 (11) (1989) 757–770. doi:10.1016/0360-5442(89)90009-1.

[34] I. H. Bell, J. Wronski, S. Quoilin, V. Lemort, Pure and pseudo-pure fluid thermophysical property evaluation and the open-source thermophysical property library coolprop, Industrial & Engineering Chemistry Research 53 (6) (2014) 2498–2508. doi:10.1021/ie4033999.

[35] J. Padet, Echangeurs thermiques, methodes globales de calcul avec exercices resolus, Université de Reims Champagne Ardenne- French Society of Heat Engineering, 2018.
URL http://www.sft.asso.fr/Local/sft/dir/user-3775/documents/Ouvrages/Padet_Ech_Thermiques/TableMatieres_Prologue.pdf

[36] R. Laskowski, The concept of a new approximate relation for exchanger heat transfer effectiveness for a cross-flow heat exchanger with unmixed fluids, J Power Technol 91.

[37] A. Triboix, Exact and approximate formulas for cross flow heat exchangers with unmixed fluids, International Communications in Heat and Mass Transfer 36 (2) (2009) 121–124. doi:10.1016/j.icheatmasstransfer.2008.10.012.

[38] A. Fakheri, Efficiency analysis of heat exchangers and heat exchanger networks, International Journal of Heat and Mass Transfer 76 (2014) 99–104. doi:10.1016/j.ijheatmasstransfer.2014.04.027.

6 Figures

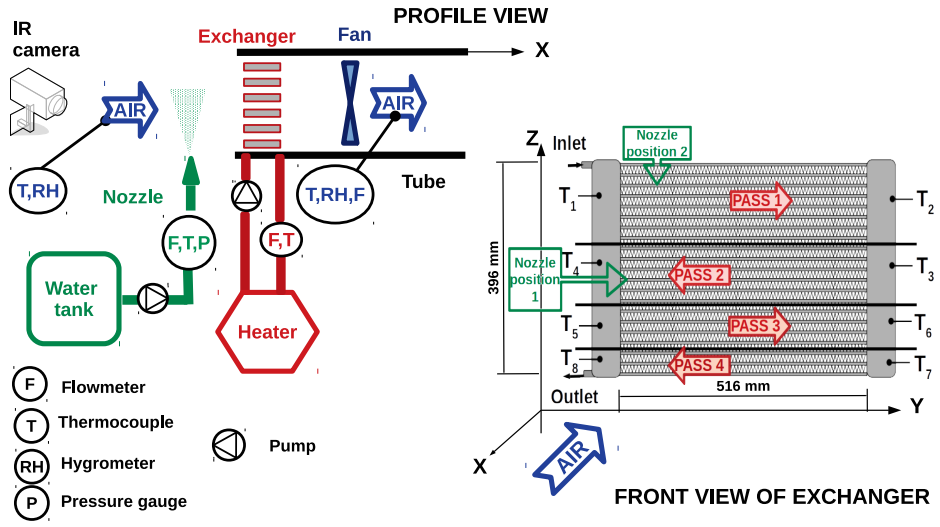

Figure 1: Experimental disposal for studying dry and wet efficiency of a heat exchanger

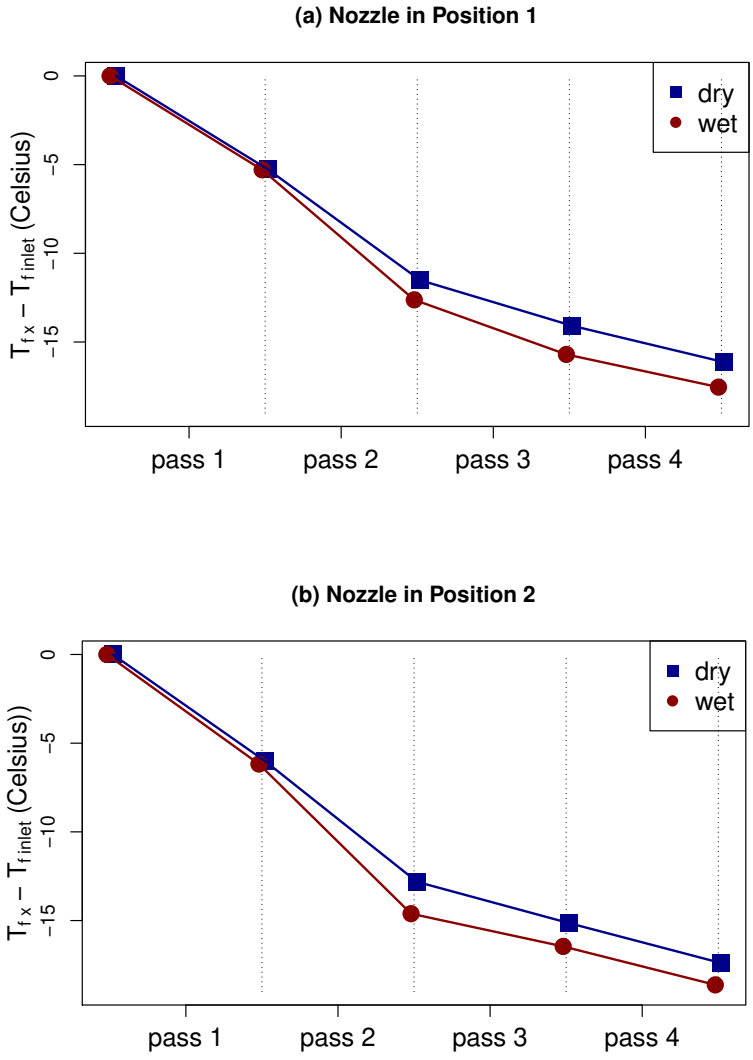

Figure 2: Fluid temperature profiles along the heat exchanger without and with spraying for nozzle position 1 (a) and nozzle position 2 (b) - $T_{f,i} = 70$ °, $m_s = 1$ L/h, $m_a = 0.2$ kg/s, $m_f = 0.078$ kg/s, $T_{a,i} = 27$ °C, $HR_{a,i} = 37\%$

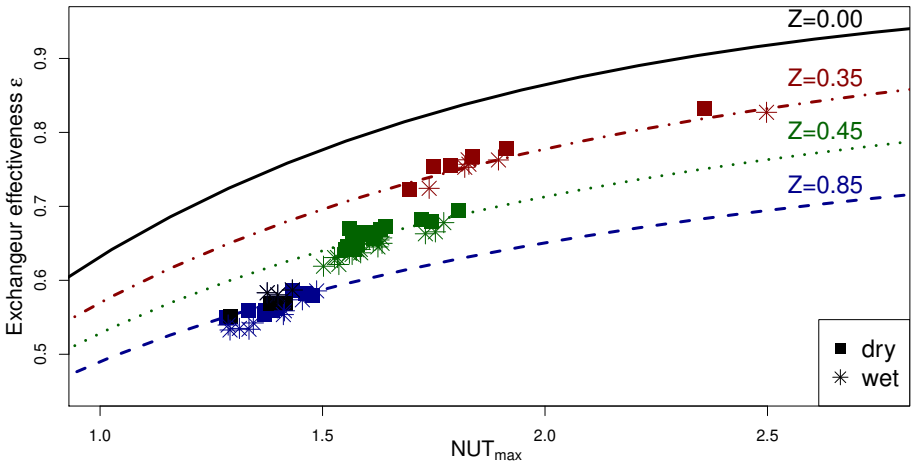

Figure 3: NTU and effectiveness of dry and wet exchanger for different calorific ratios

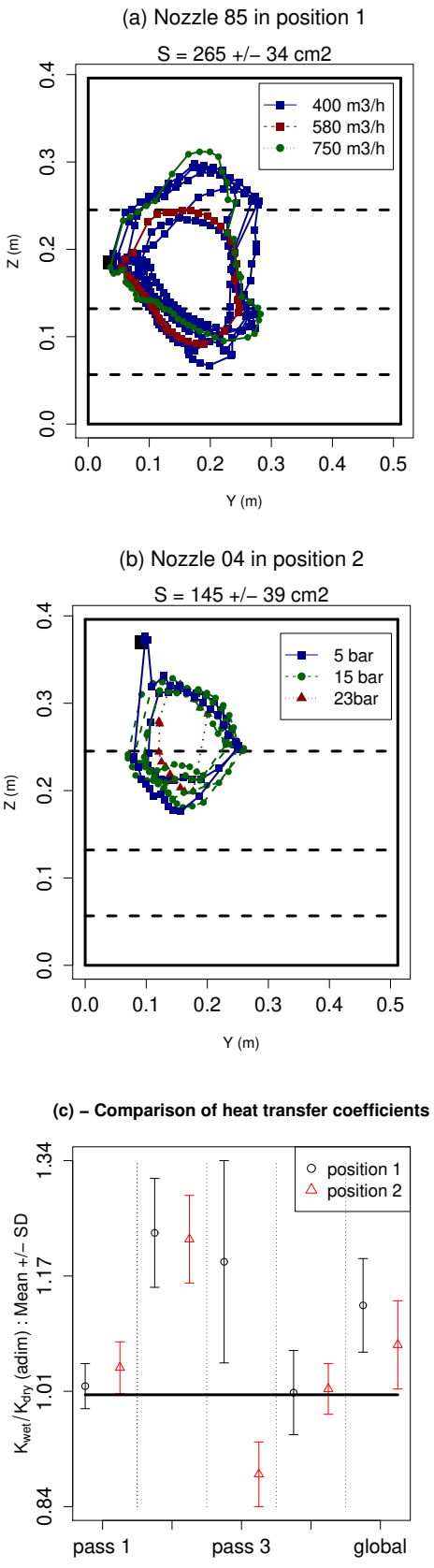

Figure 4: Impacted area for position 1 (a) and 2 (b) and (c) related changes in heat transfer coefficient for each exchanger pass

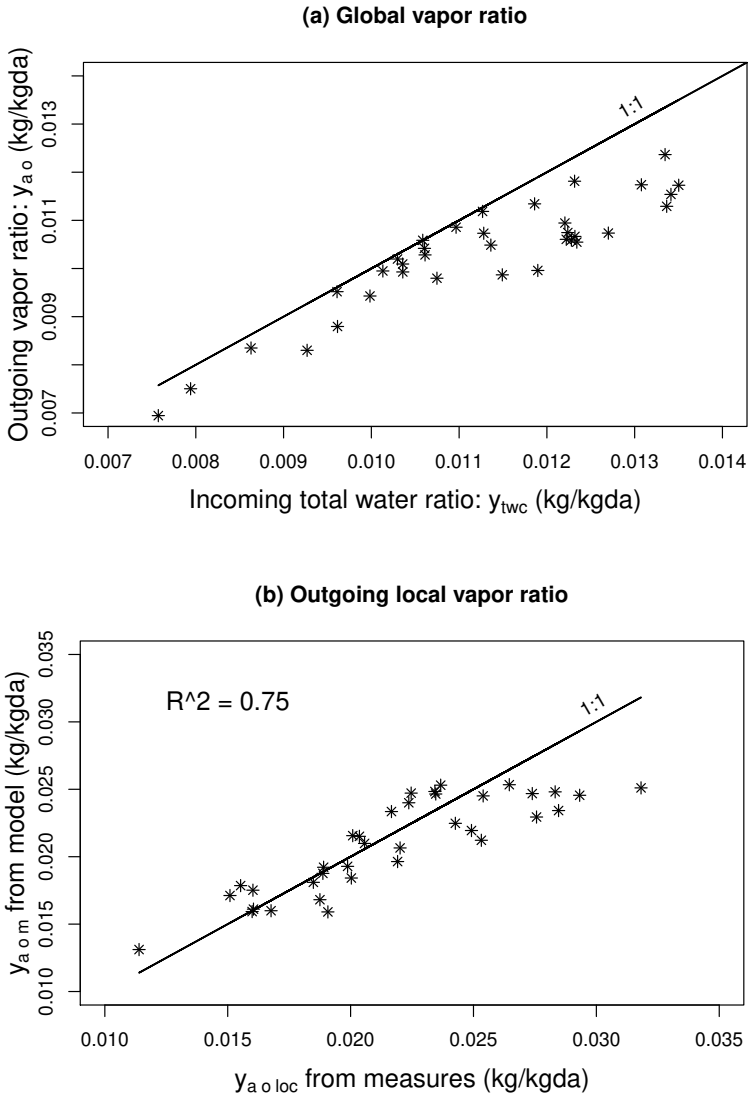

Figure 5: (a) Outgoing vapor ratio $y_{a,}$ as a function of incoming total water ratio in air and (b) modelled vapor ratio y_m versus measured one $y_{a,o,loc}$ (b)

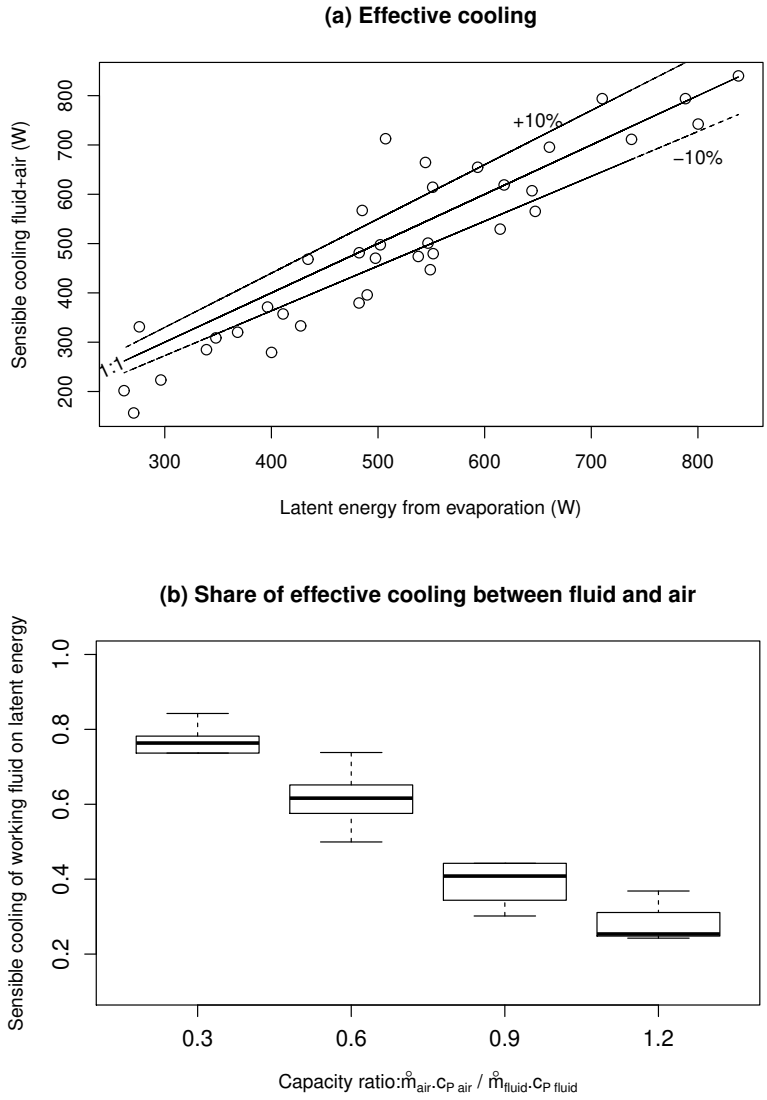

Figure 6: (a) Sensible cooling observed for air and working fluid according to the latent cooling related to evaporation rate and (b) share of sensible cooling transferred to working fluid according to the calorific ratio of the heat exchanger

7 Tables

Nomenclature

Variable			
m	flow rate (kg/s)	H	total enthalpy (W/kg/K)
C_p	specific heat (W/kg.K)	T	Temperature (°C)
ΔH_{vap}	Latent heat of vaporization (J/kg)	y	Vapor ratio (kg/kg of dry air)
R	Calorific ratio (-)	Z	Reduced calorific ratio
q	Power (W)	ϵ	Exchanger effectiveness
NTU	NUmber of Transfer unit	K	Global heat transfer coefficient ($W/m^2/K$)
S	Section (m^2)	τ	Rated values (-)
q	Heat rate (W)	τ	Rated values (-)
Subcripts and indices			
a	Dry air	max	Maximal
d	Dry condition	w	Wet condition
f	Working fluid	loc	local
s	Spray	sat	saturation
i	Inlet	sat,adia	adiabatic saturation
o	Outlet	twc	total water content
l	water,liquid	v	water,vapor
$wall$	At wall	Ex	Exchanger
m	Model		

Table 1: Energies related to the spray

	Liquid Inlet(W)	Cooling potential (W)	Cooling Effective(W)	Cooling Working fluid(W)	Cooling Air(W)	Liquid Remaining(W)	τ_f (%)
Min	26	504	259.	51	44	0.	0.24
1st Qu.	35	754	400	210	117	22	0.44
Mean	48	986	512	279	235	37	0.56
3rd Qu.	63	1142	603	324	297	54	0.65
Max	88	1531	881	637	627	84	0.84